PKCγ-Positive Neurons Gate Light Tactile Inputs to Pain Pathway Through pERK1/2 Neuronal Network in Trigeminal Neuropathic Pain Model

Wisam Dieb, DDS, MFS, PhD
Assistant Professor
Neuro-Psychopharmacology of Subcortical Dopamine Systems
University of Auvergne
Clemont-Ferrand, France

Pedro Alvarez, VD, PhD
Assistant Professor
Molecular and Clinical Pharmacology Program
Institute of Biomedical Sciences
Faculty of Medicine
University of Chile
Santiago, Chile

Aziz Hafidi, PhD
Associate Professor
Neuro-Psychopharmacology of Subcortical Dopamine Systems
University of Auvergne
Clermont-Ferrand, France

Correspondence to:
Dr Aziz Hafidi
EA7280
Neuro-Psycho-pharmacologie des Systèmes Dopaminergiques sous-corticaux
Clermont-Ferrand
F-63000, France
Email: azhafidi@univ-bpclermont.fr

Aims: To explore the possible relationship between protein kinase C gamma (PKCγ) and phosphorylated forms of extracellular signal-regulated kinases 1/2 (pERK1/2) in the rat medullary dorsal horn and the facial hypersensitivity indicative of dynamic mechanical allodynia (DMA) following chronic constriction of the infraorbital nerve (CCI-IoN). **Methods:** A well-established rat model of trigeminal neuropathic pain involving CCI-IoN was used. Facial mechanical hypersensitivity was tested with non-noxious dynamic mechanical stimulation (air-puff), and the medullary dorsal horn was examined immunohistochemically using PKCγ and pERK1/2 as pain markers. Statistical analysis was performed using Student *t* test or one-way analysis of variance (ANOVA). **Results:** Increased PKCγ and pERK1/2 expressions within the medullary dorsal horn were associated with DMA following CCI-IoN. A segmental network composed of PKCγ-positive cells located in medullary dorsal horn laminae II/III, contacting more superficially located pERK1/2-expressing cells, was identified. Ultrastructural analysis confirmed the presence of PKCγ to pERK1/2-positive cells. Moreover, intracisternal administration of the selective PKCγ inhibitor KIG31-I blocked both the DMA and pERK1/2 expression in a dose-dependent manner. Although the number of pERK1/2-positive cells was significantly elevated with air-puff stimulation, DMA rats not receiving air-puff stimulation showed significant pERK1/2 expression, suggesting they were experiencing spontaneous pain. **Conclusion:** PKCγ cells in the medullary dorsal horn may be involved in DMA following CCI-IoN through the activation of pERK1/2-expressing cells, which then may relay non-nociceptive information to lamina I cells in the medullary dorsal horn. *J Oral Facial Pain Headache 2015;29:70–82. doi: 10.11607/ofph.1353*

Key words: *chronic constriction of infraorbital nerve, dynamic mechanical allodynia, neuropathic pain, protein kinase C gamma*

Neuropathic pain is a disabling condition and an important source of chronic pain that remains a considerable therapeutic challenge. Some of the more severe forms of neuropathic pain are those affecting the trigeminal territory and include trigeminal neuralgia, posttraumatic neuropathic pain, and postherpetic neuralgia. Among the symptoms observed in patients affected by trigeminal neuropathic pain, the most disturbing may be those produced by dynamic mechanical allodynia (DMA). This symptom, defined as pain produced by a normally non-noxious stimulus, can be triggered by routine activities such as shaving, teeth cleaning, chewing, talking, or even exposure to air currents, and it considerably reduces the patient's quality of life.[1] Unfortunately, the treatment of DMA is often unsatisfactory, mostly due to the limited efficacy of currently available drug therapies. Therefore, understanding the cellular and molecular events underlying DMA is a prerequisite for the development of rational analgesic strategies.

Protein kinase C gamma (PKCγ) and phosphorylated forms of extracellular signal-regulated kinases 1/2 (pERK1/2) are known to play an important role in neuropathic pain. In spinal and medullary dorsal horns, PKCγ is expressed and restricted to neurons of their superficial laminae (II and III).[2] These neurons are involved in processing nociceptive information and participate in the chronicity of pain.[3–7] pERK1/2 is expressed in the dorsal horn as a result of noxious stimulation.[8–11] Its

phosphorylation is implicated in pain[12] and its pharmacologic blockade reduces pain behavior after chronic constriction injury of the infraorbital nerve (CCI-IoN).[13] ERK1/2 phosphorylation promotes central sensitization by altering the regulation of glutamate receptors and potassium channel activities.[12] It plays a pivotal role in the development of thermal and mechanical hypersensitivity after trigeminal nerve injury[14] and following peripheral inflammation.[9,11]

Although both molecules are implicated in neuropathic pain, the relationship between the cell subtypes that express these markers has not yet been investigated. Therefore, the aim of this study was to explore the possible relationship between PKC and pERK1/2 in the rat medullary dorsal horn (MDH) and the facial hypersensitivity indicative of DMA following CCI-IoN. Since neither PKCγ nor pERK1/2 have ever been explored together in this neuropathic pain model, the expression of both markers was first explored in the MDH of allodynic rats and compared to that of non-allodynic and sham rats. Secondly, the effects of PKCγ inhibition on the expression of pERK1/2 and DMA were investigated by the intracisternal injection of a selective PKCγ inhibitor (KIG31-1). Thirdly, PKCγ cell process projections to pERK1/2 cell subtypes in the MDH were examined at the light microscopic and ultrastructural levels.

Materials and Methods

Animals

Adult male Sprague-Dawley rats (250 to 350 g; n = 72) were obtained from Charles River Laboratories (L'Arbresle, France) and maintained in a controlled environment (lights on 08:00 to 20:00 hours, 22°C) with food and water freely available. They were housed three to four per cage. Every effort was made to minimize the number of animals used. The experiments conformed to the ethical guidelines of the International Association for the Study of Pain and the European Community Council directive of 24 November 1986 (86/609/EEC). All the experimental procedures were approved by the local institutional animal care and use committee (Université Clermont 1).

Surgery

CCI-IoN was performed following an established surgical procedure.[6,13,15] Briefly, an incision approximately 1 cm long was made along the gingivobuccal margin, begun just proximal to the first molar, in 36 rats. About 0.5 cm of the IoN was freed of adhering tissue, and two ligatures (4-0 chromic gut) separated by a 1- to 2-mm interval were tied loosely around it using 4-0 chromic gut. In the other 36 rats, a sham operation was performed that was identical to that in CCI-IoN rats except that the nerve was not ligated.

Behavioral Testing and Analysis

This study focused on allodynia and not hyperalgesia; therefore, a mild (air-puff) non-noxious stimulus was used. The stimulus was applied by a blinded experimenter every 3 minutes on the vibrissal pad (IoN territory). Each series of stimulations consisted of five von Frey filament (2 g) applications every 5 seconds, alternatively, on each side of the face. Behavioral responses were scored according to the method of Vos et al[16]: *(1)* detection (rat turns its head toward stimulus); *(2)* withdrawal reaction (rat turns its head away); *(3)* escape/attacks (rat avoids further contact with the stimulus, or attacks the filament); *(4)* asymmetric grooming (rat displays an uninterrupted series of at least three wash strokes directed to the stimulated area). An absence of response corresponded to a zero score. A mean score value was then calculated for each stimulation series. All the rats (n = 24) were subjected to 13 sessions of behavioral testing at different time points: before surgery (day 1) and after surgery, on weeks 1 through 12.

Intracisternal Injections

After brief (< 3 minutes) anesthesia with 2% halothane, CCI-IoN and the sham rats received intracisternal administrations[17] of KIG31-1 (50 or 100 pmoles, dissolved in 5 µL vehicle; KAI Pharmaceuticals) or the vehicle alone (5 µL, Tat carrier). Following recovery (< 2 minutes), the rats (n = 15) were placed in the observation field (24 × 35 × 18 cm). Gentle air-puffing (1-second duration) was applied every 3 minutes onto the center of the vibrissal pad by using a calibrated pump.

KIG31-1 is devoid of unspecific psychomotor effects.[18] It is conjugated to Tat, a peptide carrier, via a cysteine-cysteine bond at its N terminus. KIG31-1 competes with activated PKCγ for binding to the isoenzyme-specific docking proteins, which are receptors for activated C kinase. Covalent linking of KIG31-1 to the Tat molecule enables efficient transfer of the peptide into cells.

Immunohistochemical Analysis and Cell Count

After postoperative day 21, CCI-IoN and sham rats were deeply anesthetized with urethane (1.5 g/kg IP). Twenty minutes after the induction of anesthesia, the CCI-IoN and sham rats (n = 33) were stimulated for 2 minutes in the ipsilateral infraorbital region by gentle air-puffing (60 stimuli delivered, 0.5 Hz). Three minutes after the end of the stimulation, the rats were perfused transcardially by a cold (10°C) phosphate-buffered solution (0.1 M, pH 7.6), containing 4% paraformaldehyde and 0.03% picric acid, for 15 minutes. The brain was placed in a 30% sucrose and 0.05% sodium azide solution overnight at 4°C. Coronal sections, 30-µm thick, were cut on a freezing microtome and collected in 0.05 M tris-buffered saline (TBS).

Free-floating brainstem sections were placed in 1% normal goat serum for 1 hour before overnight incubation at room temperature in primary antibody solutions (mouse and rabbit anti-pERK1/2 [1:1,000, Cell Signaling Technologies], mouse and rabbit anti-PKCγ [1:4,000, Sigma-Aldrich and Santa Cruz]). The corresponding secondary antibodies (1:400 for goat anti-mouse Cy3, 1:200 for goat anti-rabbit Cy2) were incubated at room temperature for 3 hours. All antibodies were diluted in TBS containing 0.25% bovine serum albumin and 0.3% Triton X-100. The sections were finally rinsed in TBS, mounted on gelatin-coated slides, dehydrated in alcohol, cleared in xylene, and coverslipped with DPX (distrene, plasticizer, xylene) mounting medium. The specificity of the immunostaining was assessed by omitting the primary antibodies, which resulted in the absence of signal.

Fluorescence was analyzed by using a motorized Zeiss Axioplan 2 microscope equipped with a Hamamatsu C4742-95 digital camera driven by MetaMorph 5.4 software. In each rat, image acquisition and fluorescent signal quantification were performed on seven different sections, each taken at a given rostrocaudal plane within the MDH (from 0 to −2,160 μm at 360-μm intervals). Brainstem sections were categorized according to their approximate rostrocaudal location from the MDH/trigeminal subnucleus interpolaris junction. The pERK1/2-positive cells were counted according to their location in the different MDH laminae from sections co-stained for PKCγ, a cellular marker that highlights the inner lamina II (IIi).[2] The delineation of the MDH was based on the Paxinos and Watson atlas.[19] The data are expressed as the sum of the total number of labeled cells counted from all sections that were analyzed in each animal in both the stimulated and nonstimulated groups.

The tissue-processing technique used for the electron microscopy has been described previously.[20] Briefly, the MDH was cut into 40-μm-thick sections by using a vibratome and processed sequentially for PKCγ and pERK1/2 immunohistochemistry. After PKCγ diaminobenzidine (DAB) reaction, the sections were incubated with the rabbit anti-pERK1/2 antibody for 3 hours, rinsed several times with TBS, and incubated with an anti-rabbit gold-conjugated antibody 1:200 (Sigma-Aldrich) for 2 hours. Sections were rinsed several times and postfixed for 1 hour in 1% OsO_4. After dehydration in a graded acetone series, the sections were incubated overnight in a mixture of acetone and Epon resin (1:1). The samples were transferred to Epon for 2 hours, flat-embedded between sheets of Aclar plastic, and incubated overnight at 60˚C. The MDH was cut from Aclar sheets, capsule-embedded with Epon, and stored at 60˚C overnight. Ultrathin sections (85 nm) were prepared from Epon blocks, sampled for electron microscopy, and collected on nickel grids. The sections were examined with a JEOL 1200EX electron microscope, and pictures were acquired at 10,000X magnification by using a CCD (charge-coupled device) camera (AMT).

Statistical Analysis

The results are expressed as mean ± SEM. Statistical analysis was performed using Student *t* test, or one-way analysis of variance (ANOVA) followed by a post-hoc Student-Newman-Keuls test or one-way repeated-measures (RM) ANOVA followed by a post-hoc Student-Newman-Keuls test. Correlation coefficients were calculated by linear regression analysis. The level of significance was set at $P < .05$.

Results

Dynamic Mechanical Allodynia Behavior

Based on the score related to their nociceptive responses to air-puff stimuli, the rats were divided into three groups (Fig 1): *(1)* rats that developed DMA after CCI-IoN ("allodynic"), *(2)* rats subjected to CCI-IoN that did not develop DMA ("non-allodynic"), and *(3)* control rats that were operated without CCI-IoN ("sham"). The highest allodynic score was observed between the second and third week postsurgery (Fig 1), and so the pharmacologic studies were performed at 2 weeks after the surgery and the immunohistochemical analysis at 3 weeks after the surgery.

Ipsilateral to the IoN injury, an increase in the nociceptive score of the allodynic rats was observed 1 week after the surgery, but the increase was not statistically significant (Fig 1, $P > .05$). During the second and third week postsurgery, the increase in the nociceptive score became significant compared to the non-allodynic and sham groups (Fig 1, $P < .001$). As observed in the allodynic rats, the non-allodynic rats exhibited a trend of enhanced nociceptive score values during the first week after surgery (Fig 1, $P > .05$). The sham group did not show any significant variation in the average score after surgery when compared to presurgery.

Similar results were obtained when air-puff stimuli were delivered on the contralateral side: 1 week after surgery the average score was significantly higher in the group of allodynic rats when compared to sham animals (Fig 1, $P < .01$). At 2 and 3 weeks postsurgery, this score remained significantly higher in allodynic animals (Fig 1, $P < .001$), reaching values comparable to those obtained by stimulation of the ipsilateral region.

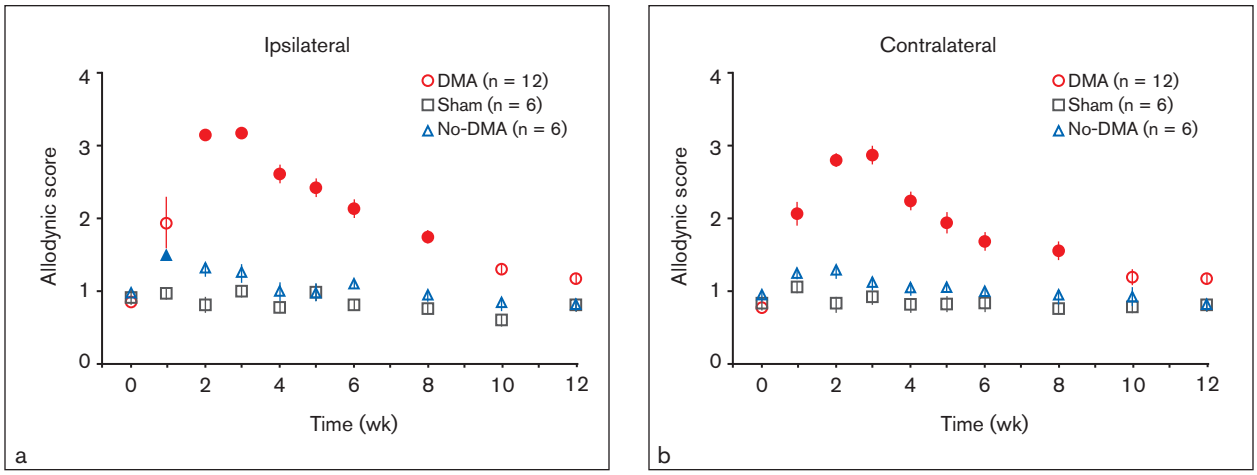

Fig 1 Time course of dynamic mechanical allodynia. The graph represents data from three animal groups: allodynic (DMA, circle), non-allodynic (No-DMA, triangle), and sham (square) for ipsilateral and contralateral allodynic behavior following CCI-IoN or sham surgery. At 1 week postsurgery, the DMA group began to show signs of allodynic behavior evoked by ipsilateral and contralateral stimulation when compared to No-DMA and sham groups. However, this change was significant ipsilaterally at 14 days postsurgery, and it reached its highest score after 3 weeks and lasted up to 8 weeks. Allodynic behavior evoked by contralateral stimulation was significant at 1 week postsurgery and was similar to that evoked by the ipsilateral stimulation by 3 weeks postsurgery. The sham group showed no significant change in behavioral score. Solid figures represent significant differences in comparison to sham animals ($P < .001$).

Involvement of PKCγ-Positive Cells in Dynamic Mechanical Allodynia

Consistent with previous studies,[2,6] PKCγ immunostaining was mainly observed in lamina IIi of the MDH, ipsilateral (Figs 2a, 2d, and 2g) and contralateral (Figs 2b, 2e, and 2h) to the IoN injury. There were significant increases in staining intensity (lamina IIi) and the numbers of PKCγ-positive cells (lamina III; $P < .001$) in allodynic animals compared to sham and non-allodynic rats. Further investigations revealed the presence of contacts between these PKCγ-positive cells (Figs 2j to 2l). These cells were organized in clusters of three to four cells ventrodorsally oriented from deep lamina III through lamina IIi. Most of the superficial cells of these clusters were in contact with PKCγ cells of lamina IIi (Fig 2l).

The number of PKCγ-positive cells in lamina III increased bilaterally in allodynic rats compared to non-allodynic (Fig 3, $P < .001$) and sham animals (Fig 3, $P < .001$). No significant difference in PKCγ staining intensity was observed between the non-allodynic and sham groups.

Quantitative analysis of PKCγ immunofluorescence within lamina IIi showed a significant increase in its intensity in allodynic rats in comparison to non-allodynic rats (Fig 3, $P < .001$) and sham rats (Fig 3, $P < .001$). No significant difference was observed between non-allodynic rats and sham rats ($P > .05$). The results of PKCγ immunofluorescence analysis from ipsilateral and contralateral MDH were similar.

Air-Puff–Induced pERK1/2 Expression in MDH Laminae

Consistent with previous studies,[10,13,14] pERK1/2 staining was observed in cells located mainly in the superficial MDH laminae I and II (both outer lamina II [IIo] and IIi), although some positive cells were also observed in deeper laminae (Fig 4a) in rats exhibiting DMA. At higher magnification, the staining was located in the cell somata, nucleus and processes, and these positive cells showed morphological features characteristic of neurons, such as thick dendrites branching into thinner processes and thin processes of constant diameter indicative of axons (Figs 4b to 4d). The pERK1/2-positive cells were generally observed in clusters of two or more adjacent cells, exhibiting contacts between each other (Figs 4e to 4g). These contacts were observed between pERK1/2-positive cells within the same lamina, between cells located in sub-laminae IIi and IIo, and between cells in laminae IIo and I (Figs 4e to 4g).

Air-puff stimuli evoked pERK1/2 activation resulting in a gradient in the total number of pERK1/2-expressing cells, in the following order: allodynic > nonallodynic > sham rats (Fig 5). There was no significant difference in the number of pERK1/2 cells between the non-allodynic rats and the sham animals ($P > .05$).

In the stimulated allodynic rats, most of the pERK1/2-positive cells were observed in the superficial laminae I and II, ipsilateral and contralateral to

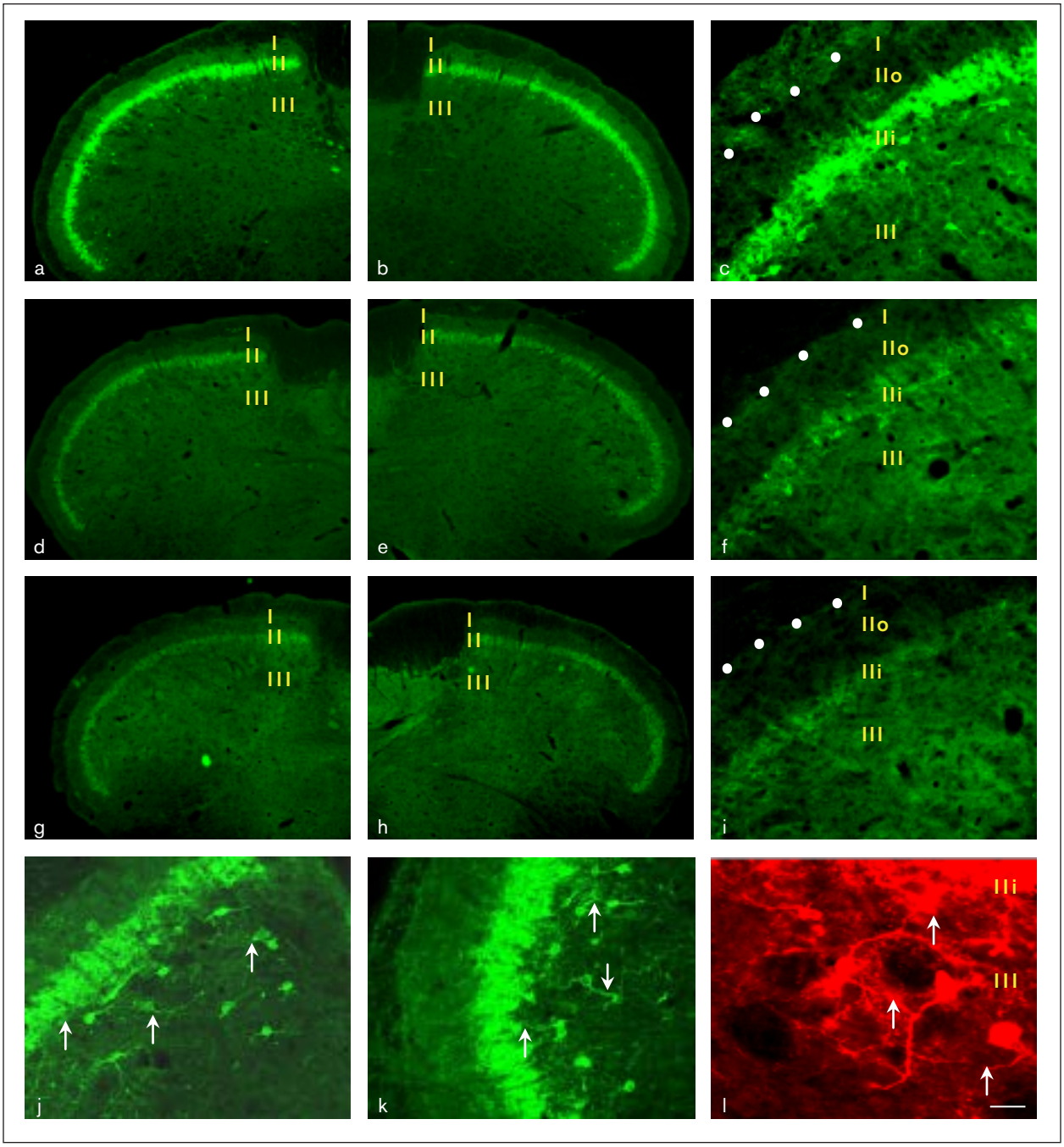

Fig 2 Very intense PKCγ immunolabeling was observed in the MDH of **(a to c)** allodynic rats following CCI-IoN compared to **(d to f)** non-allodynic and **(g to i)** sham rats. Intense labeling was observed in lamina IIi cells and in scattered cells within lamina III, and only a few cells were present in the external area of lamina II. Intense PKCγ staining was present in allodynic rats in both ipsilateral and contralateral MDH, which contrasts with the weaker PKCγ staining observed in the MDH of non-allodynic and sham rats. Only a slight difference in nuclear staining occurred between non-allodynic and sham rats. At high magnification, a gradient of PKCγ staining was observed between **(c)** allodynic, **(f)** non-allodynic, and **(i)** sham rats. Note that PKCγ labeling in non-allodynic rats was slightly higher than in sham rats but far less intense when compared to the allodynic rats. There was a high increase of PKCγ staining in lamina III **(j to l)**. In addition, the positive cells presented contacts with each other *(white arrows)* within this lamina and with PKCγ cells in lamina IIi **(l).** Scale bar = 200 μm in a, b, d, e, g, and h; 50 μm in c, f, i, j, and k; and 10 μm in l.

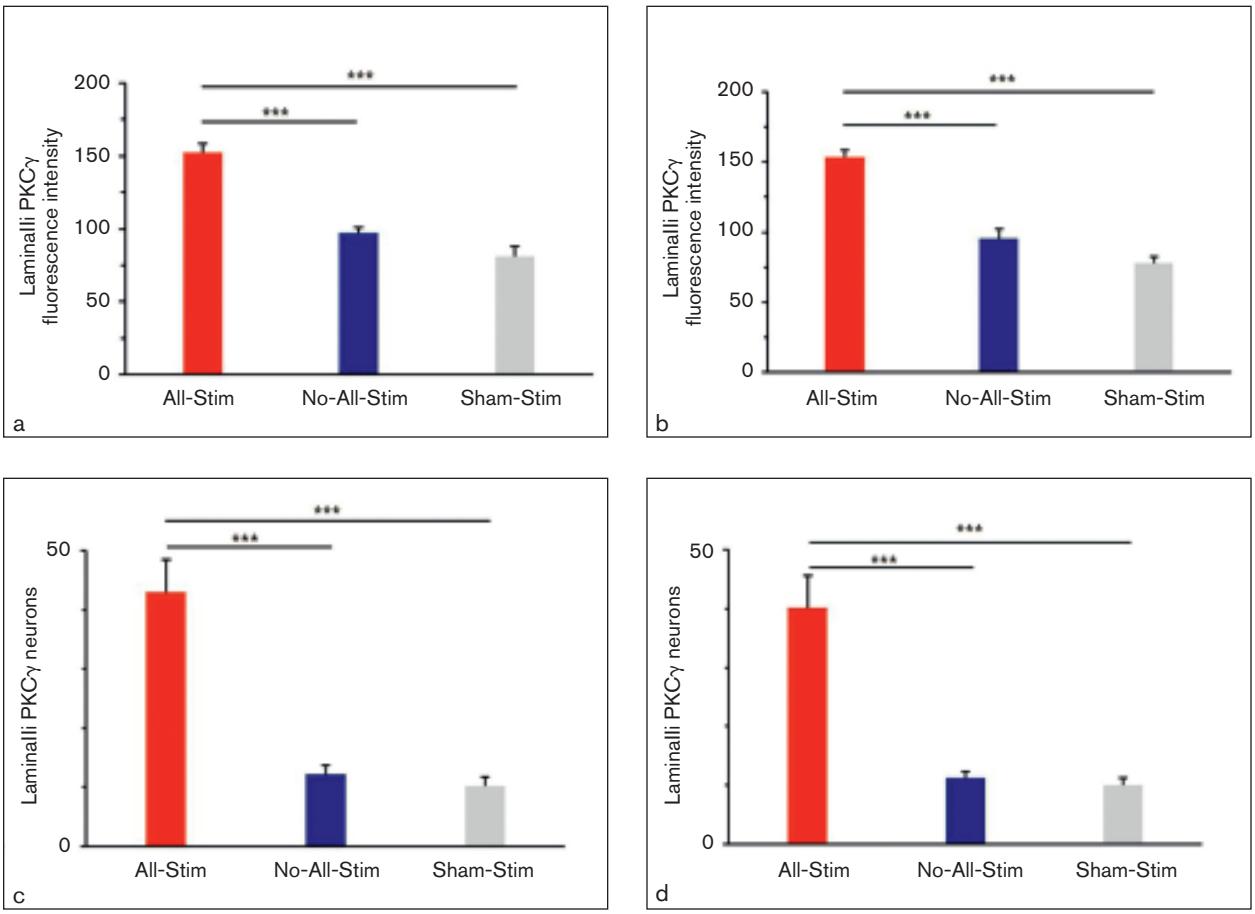

Fig 3 Quantification of PKCγ expression and cell counts in the MDH of allodynic rats. Image analysis quantification from lamina IIi revealed a highly significant ($P < .001$) difference in the intensity of staining between allodynic and non-allodynic and sham rats **(a)**. This difference was observed in both ipsilateral and contralateral MDH following CCI-IoN **(b)**. The cell count of PKCγ-positive cells in lamina III demonstrated a significant ($P < .001$) increase in their number in both **(c)** ipsilateral and **(d)** contralateral MDH of allodynic rats in comparison to non-allodynic and sham rats. ***$P < .001$.

CCI-IoN (Fig 5). Lamina II (IIi and IIo) contained the largest number of pERK1/2-immunopositive cells, which had increased considerably in the allodynic rats in comparison to the non-allodynic and sham groups (Fig 5). pERK1/2 expression in ipsilateral laminae I and II (IIi and IIo) had increased considerably in the allodynic rats in comparison to the non-allodynic and sham rats (Fig 5a, $P < .001$). Comparable results were obtained on the contralateral side, especially in lamina II, where pERK1/2 expression had increased markedly in comparison to the non-allodynic and sham rats ($P < .001$). The number of pERK1/2- positive cells in the contralateral lamina I of the allodynic rats was significantly higher in comparison to the non-allodynic and sham rats, but to a lesser degree than that observed in the ipsilateral side (Fig 5b, $P < .01$). In laminae III-IV and V, the number of pERK1/2-positive cells, ipsilateral or contralateral to the operated IoN, was not different in the allodynic rats in comparison to the sham rats. Finally, no significant differences in pERK1/2 expression were observed between the non-allodynic and sham groups (Figs 5a and 5b, $P > .05$).

Spontaneous and Evoked pERK1/2 Expression

To determine whether pERK1/2-positive cells represented evoked or spontaneous activation of nociceptive pathways after IoN injury, the authors compared their expression in stimulated and non-stimulated allodynic rats (Fig 5). In the ipsilateral MDH, a higher number of pERK1/2-positive cells was observed in laminae I, IIo, and IIi of the stimulated rats compared to the non-stimulated rats (Fig 5a; $P < .001$, $P < .01$, and $P < .05$, respectively). Similar results were obtained in the contralateral MDH (Fig 5b, $P < .01$).

A high correlation between the allodynic score and the number of pERK1/2-positive cells was observed (Fig 6), the correlation coefficient being higher in the ipsilateral compared to the contralateral MDH ($r = 0.69$ [$P = .004$] and 0.60 [$P = .024$], respectively).

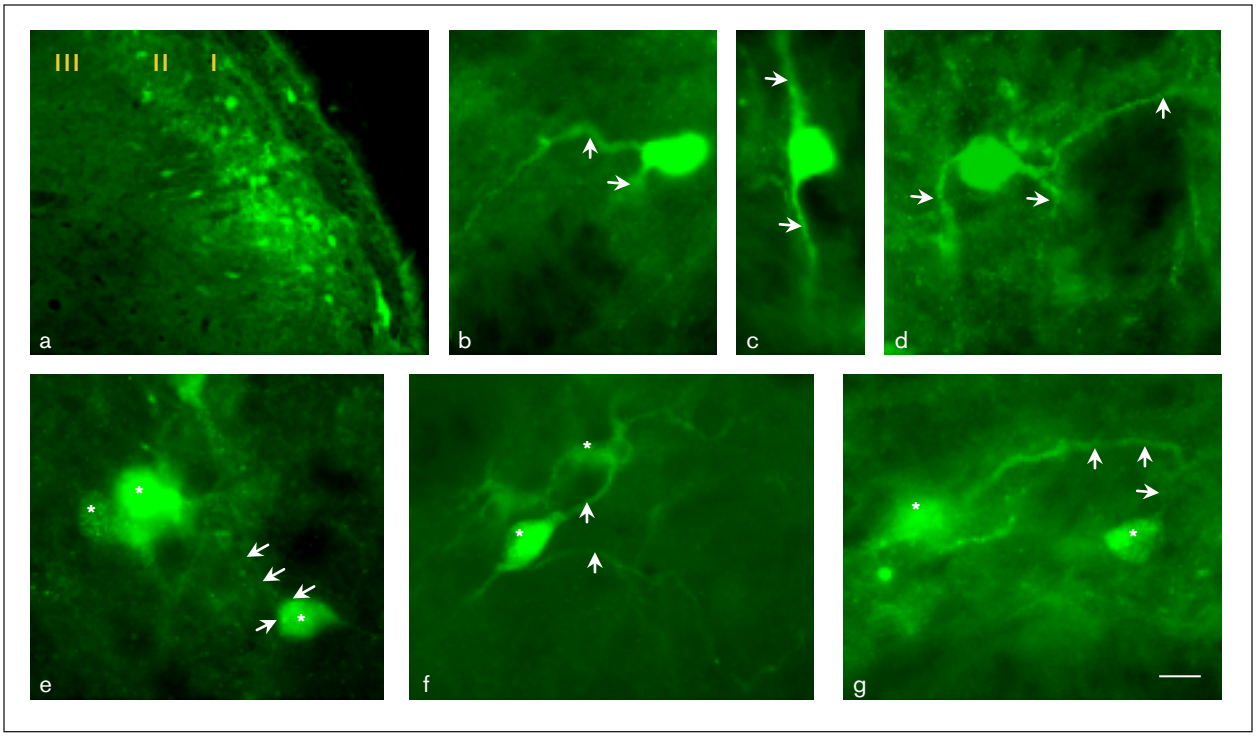

Fig 4 Air-puff–induced pERK1/2 expression in the MDH. **(a)** pERK1/2 staining was observed in the superficial layer cells (I, II, III) of the MDH following CCI-IoN. **(b to d)** At high magnification, pERK1/2-positive cells showed morphologic features characteristic of neurons and had intense staining in their somata *(stars),* nucleus, and processes *(arrows)* in **(c)** lamina IIo and **(d)** lamina I. **(e to g)** Positive cells presented contacts *(arrows)* with each other. Scale bar = 50 µm in a, and 10 µm in b to g.

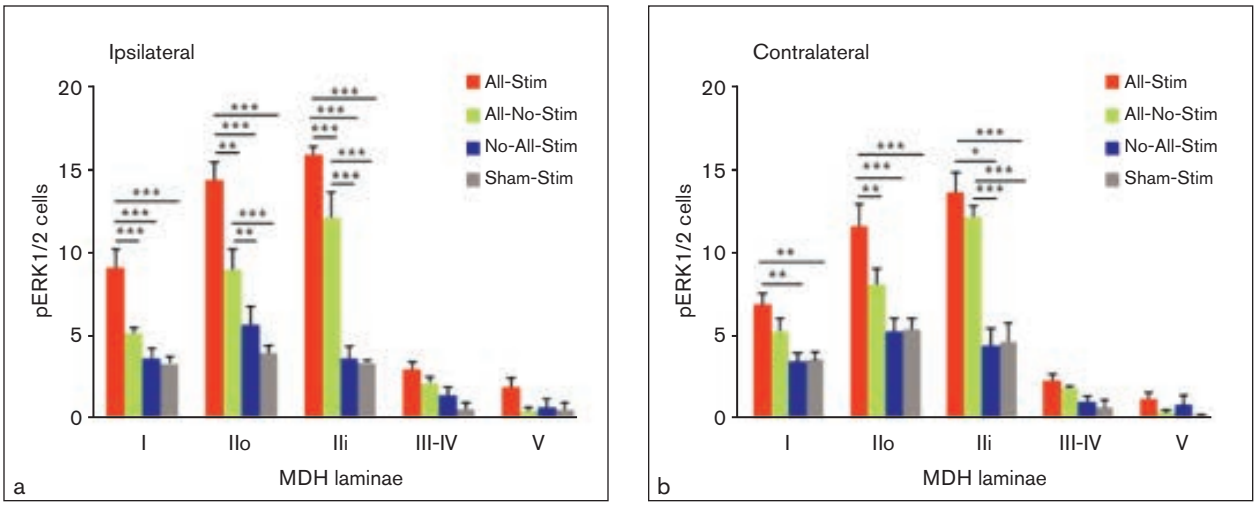

Fig 5 **(a)** Number of pERK1/2-positive cells in the MDH ipsilateral to the CCI-IoN. Four groups of animals were investigated: allodynic-stimulated (All-Stim) and nonstimulated (All-No-Stim), non-allodynic stimulated (No-All-Stim), and sham-stimulated (Sham-Stim). The number of pERK1/2-positive cells in all the MDH laminae of the allodynic subgroups was higher in comparison to the sham rats. This increase in number was highly significant ($P < .001$) in the MDH lamina I and lamina II (IIi, IIo) only. There was also a significant difference in the number of pERK1/2-positive cells between allodynic-stimulated and nonstimulated groups. The former showed the highest number of pERK1/2-positive cells. **(b)** In the contralateral MDH, a similar increase occurred in the number of pERK1/2-positive cells to that of the ipsilateral side. A comparative analysis revealed a significant ($P < .001$) increase in the number of pERK1/2-positive cells in lamina II (IIi, IIo) of the allodynic-stimulated group. This increase was not significant in the other laminae of this animal group. In the allodynic-nonstimulated group, the increase of pERK1/2 was significant only in lamina IIi. Bars represent standard deviation. *$P < .05$; **$P < .01$; ***$P < .001$.

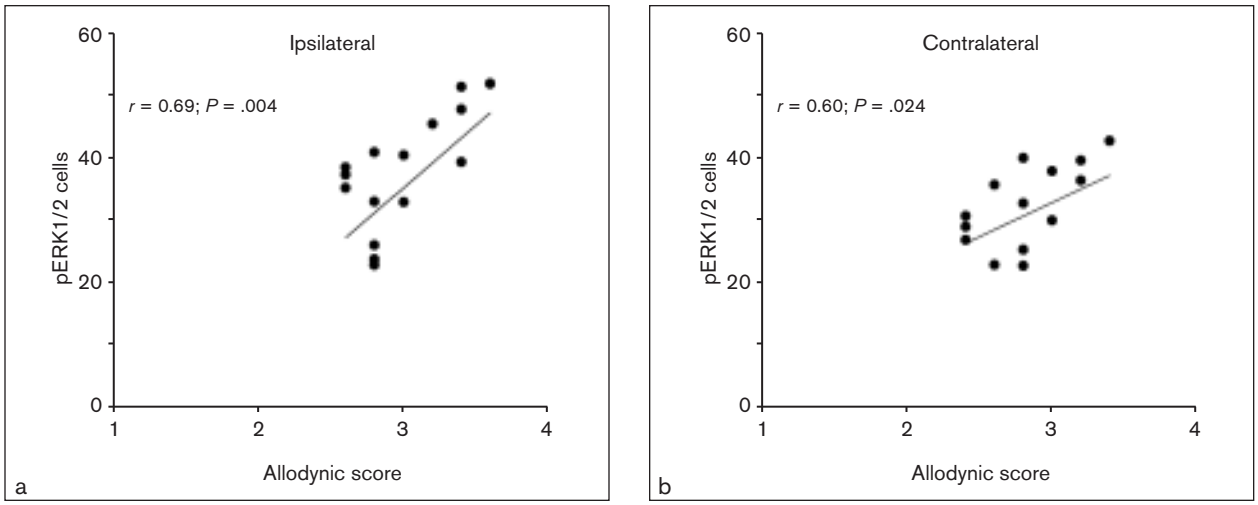

Fig 6 Correlation between pERK1/2 expression and allodynic score. There was a high correlation between the total numbers of pERK1/2-positive cells in the MDH and the severity of the allodynia in both the **(a)** ipsilateral and **(b)** contralateral MDH following CCI-IoN. The highest number of pERK1/2-positive cells was observed in both the ipsilateral and contralateral MDH in animals that also had high allodynic behavioral scores. This correlation was greater for the ipsilateral side ($P = .004$) than the contralateral side ($P = .024$). The slope of the curve was higher on the ipsilateral side ($r = 0.69$) compared to the contralateral side ($r = 0.60$).

Lack of pERK1/2 and PKCγ Co-expression

As shown in Figs 7a to 7c, pERK1/2 and PKCγ did not co-localize in allodynic rats. However, detailed analysis revealed the presence of PKCγ-positive processes ending on the surface of pERK1/2-positive neurons (Figs 7g to 7l, *arrows*). PKCγ projections on pERK1/2-positive neurons were observed in laminae IIi and IIo. Ultrastructural investigations (Figs 8a to 8c) confirmed the light microscopic observations, with PKCγ contacts (DAB reaction) found in apposition to the plasma membrane of pERK1/2-positive (gold particles) somata (Fig 8c). In these examples (pERK1/2-positive cell from lamina IIo), the gold dots indicate the distribution of pERK1/2, which was highly concentrated within the cytoplasm along the nuclear membrane and within the nucleus.

Inhibition of PKCγ Attenuates Both DMA and pERK1/2 Expression

Intracisternal administration of KIG31-1, a specific PKCγ antagonist in CCI-IoN rats, produced a dose-dependent attenuation of DMA (Figs 9a and 9b). In the case of the 100-pmol dose, a dramatic inhibition of DMA was observed, an effect that lasted for up to 5 hours (Fig 9a). The injection of aCSF (data not shown) and Tat carrier did not have any effect on DMA.

Twenty minutes after intracisternal injection of KIG31-1, the allodynic rats received air-puff stimuli and their brains were rapidly processed for immunohistochemistry. As shown in Fig 10a, a general decrease in pERK1/2 expression throughout the ipsilateral MDH was observed. This significant diminution was observed in the ipsilateral lamina I ($P < .01$) and laminae IIo ($P < .001$) and IIi ($P < .001$). Similarly, a significant decrease in the number of pERK1/2-positive cells was observed in the contralateral lamina II (IIi, IIo; Fig 10b).

Discussion

The major findings of this study were: *(1)* PKCγ expression in laminae IIi and III of the MDH is increased in rats exhibiting DMA following CCI-IoN. *(2)* pERK1/2 expression in the MDH superficial laminae is associated with both evoked and spontaneous pain behavior that has been previously described in this neuropathic pain model.[16] The comparison of pERK1/2 expression in CCI-IoN nonstimulated animals with sham animals demonstrated a significant difference in the number of pERK1/2 cells, which suggests that nonstimulated allodynic rats may have been experiencing spontaneous pain. *(3)* PKCγ and pERK1/2 cells in the MDH may be connected by synaptic projections. *(4)* Inhibition of PKCγ decreased the expression of DMA and pERK1/2 in the MDH. *(5)* Tactile (non-noxious) stimuli evoked DMA following CCI-IoN.

Dynamic Mechanical Allodynia After Infraorbital Nerve Injury

The data obtained in the present study are similar to previous results regarding the expression of DMA in rats with CCI-IoN.[13,15,21,22] The time course of the behavior indicative of DMA was consistent with that of the mechanical hypersensitivity previously reported in the IoN territory after CCI-IoN.[6,16,21–23] Nocifensive behavior reached its highest score by the second and

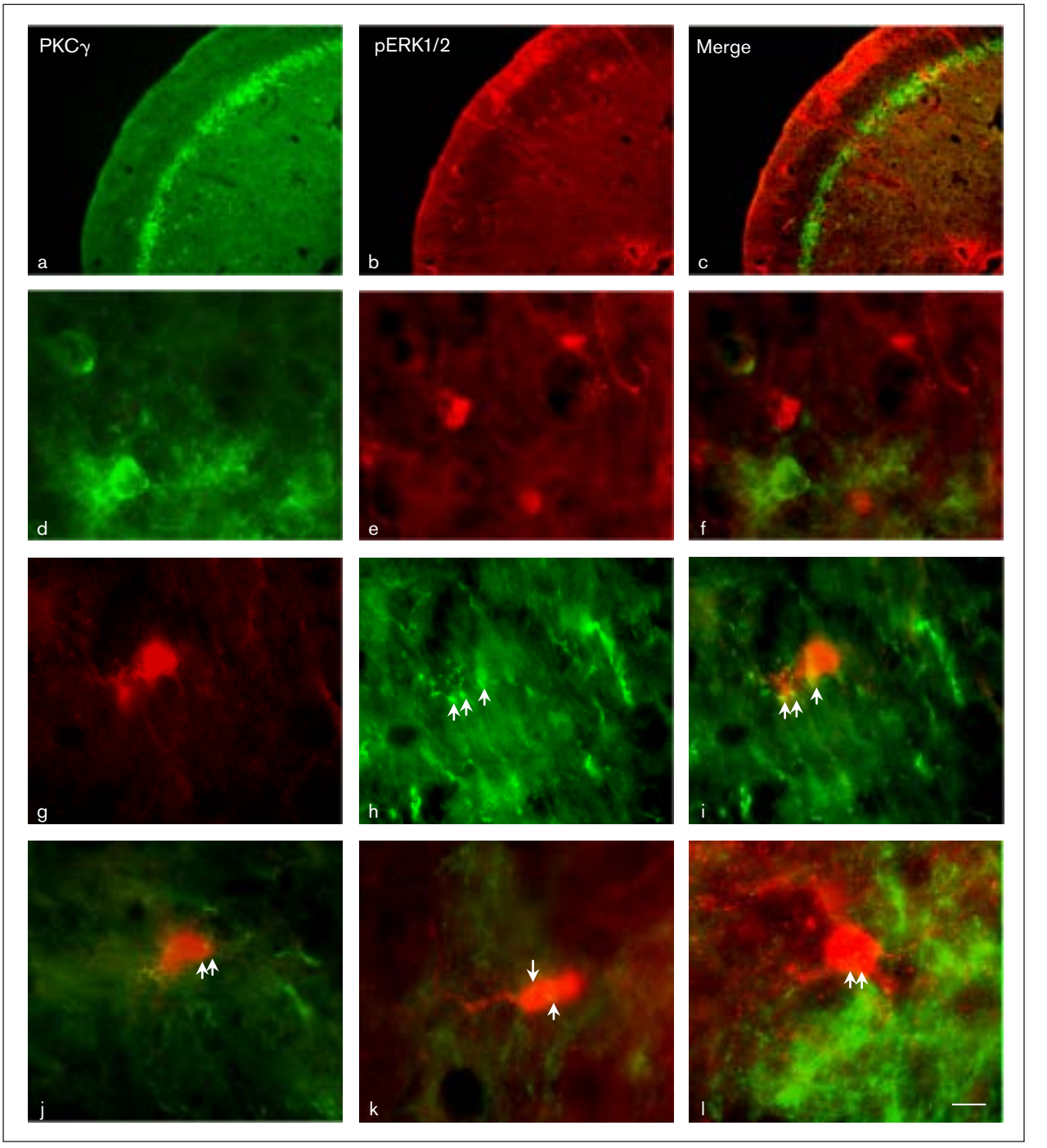

Fig 7 PKCγ and pERK1/2 are expressed in distinct cell subtypes. Double PKCγ *(green)* and pERK1/2 *(red)* labeling in MDH following CCI-IoN. **(a to c)** There was no co-localization of either marker within the same cell. **(d to f)** At high magnification, PKCγ and pERK1/2-positive cells represent distinct cell subtypes. **(g to i)** The double labeling also shows that pERK1/2-positive cells are innervated by PKCγ processes *(arrows)*. **(j to l)** Examples of pERK1/2-positive cell innervations by PKCγ processes *(arrows)*. Scale bar = 100 μm in a to c and 10 μm in d to l.

third week postsurgery in the allodynic group and decreased in the following weeks. This time course was similar for both the ipsilateral and contralateral sides. The non-allodynic group presented a significant allodynic score on the ipsilateral side only during the first week. The nocifensive behavior in this group was probably due to the inflammation resulting from the surgery. This is the first study to have explored DMA in three different groups, ie, allodynic, non-allodynic, and sham groups, for 12 weeks.

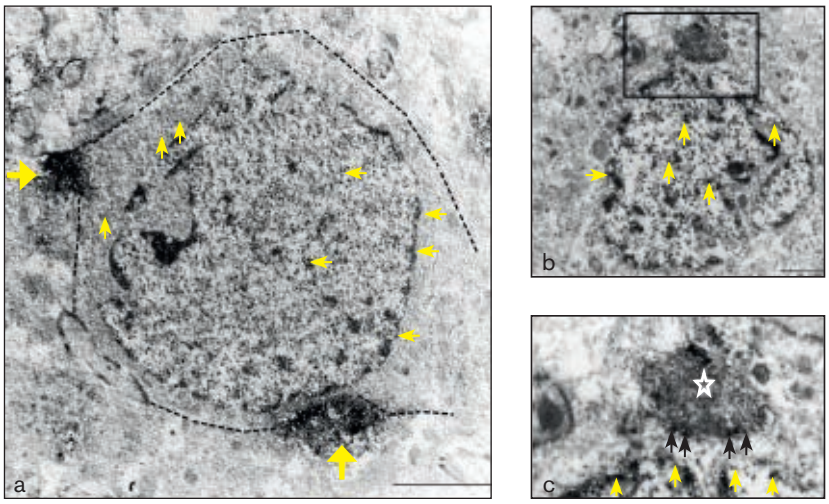

Fig 8 Ultrastructural double labeling of pERK1/2 and PKCγ. **(a to c)** Micrographs show two examples of pERK1/2-positive cells from MDH lamina IIo following CCI-IoN. The gold particles *(dots)*, which represent pERK1/2 labeling, can be observed within the nucleus along the nuclear membrane and in the cytoplasm of the cell *(thin yellow arrows)*. **(a)** pERK1/2-positive cell receives PKCγ stained endings *(thick yellow arrows)* around its soma (DAB reaction). **(b)** pERK1/2-positive cell *(thin yellow arrows)* is in contact with a PKCγ ending. **(c)** At high magnification *(square from b)*, gold particles can be observed within the nuclear membrane *(yellow arrows)*, as can a PKCγ ending *(star)*, which shows synaptic contacts *(black arrows)*. Scale bar = 2 µm.

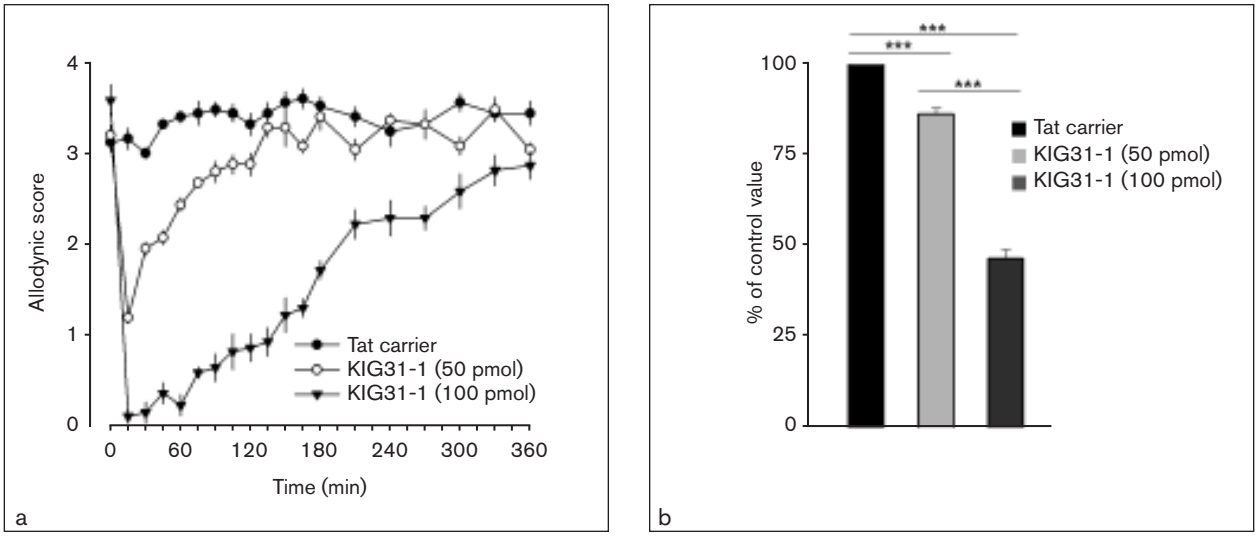

Fig 9 Selective inhibition of PKCγ blocks dynamic mechanical allodynia. **(a)** Animal behavior after intracisternal injection of two doses of PKCγ inhibitor KIG31-1 (50 and 100 pmol; n = 5 animals per dose). The transporter of the KIG31-1 Tat carrier was also injected (n = 5) as a control. The injection of Tat carrier did not have any effect on DMA following CCI-IoN. However, KIG31-1 blocked the DMA in a dose-dependent manner. DMA inhibition lasted for 6 hours. **(b)** Area under the curve for Tat carrier and the KIG31-1 injected doses. The data are reported as a percentage of the control value. There was a significant ($P < .001$) difference in the surface area under the curve between Tat carrier and both KIG31-1 concentrations (50 and 100 pmol), confirming a dose-dependent effect of KIG31-1 in the DMA. *$P < .05$; **$P < .01$; ***$P < .001$.

Following CCI-IoN, air-puff stimuli have been reported to evoke rat behaviors that are usually elicited only by nociceptive stimuli, including vigorous rubbing of the stimulated site, vocalization, attempts to escape, and aggressive behavior targeted at the source of the stimuli.[15,16,22] This suggests that CCI-IoN results in disturbed sensation, leading to the perception of light tactile stimuli as highly aversive. In the present study, this allodynia occurred ipsilateral and contralateral to the nerve injury, with the ipsilateral allodynia being more severe, as reported previously.[15,16,21,22] Contralateral pain occurs under different chronic pain conditions.[24,25] The mechanisms by which contralateral neuropathic pain occurs is still unknown, although different hypotheses have postulated that it is mediated by commissural neurons[26] or arises from altered central processing of incoming sensory information[27] or from loops involving brain and spinal cord.[28] Evidence of trigeminal primary afferent projections to contralateral MDH also has been reported.[29,30] Glial activation also has been suggested to play important roles.[26,31–33] The involvement of glia in pain on the contralateral side has been clearly demonstrated.[34,35] Clinical studies and preclinical models of neuropathic pain indicate that DMA is mediated by peripheral large myelinated Aβ fibers,[36–38] which normally convey only inputs encoding non-noxious mechanical stimulation. Air puffs have been shown to activate

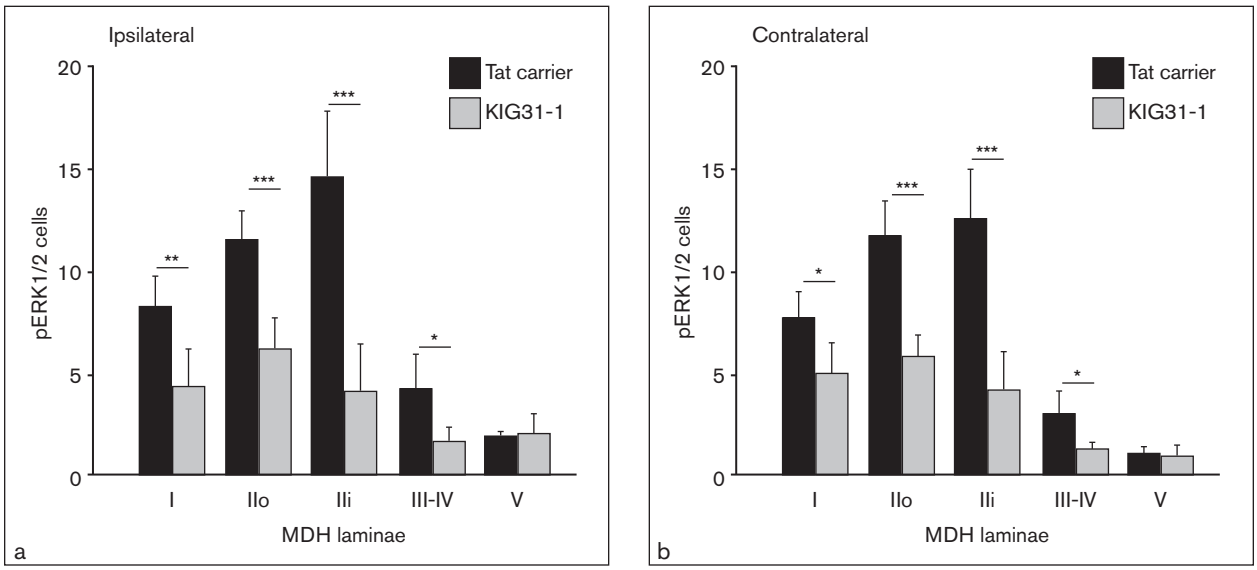

Fig 10 PKCγ inhibition depresses pERK1/2 expression. The number of pERK1/2-positive cells is shown in the MDH of allodynic animals following CCI-IoN that were injected intracisternally with KIG31-1 and Tat carrier on both **(a)** ipsilateral and **(b)** contralateral sides. A general decrease in the number of pERK1/2-positive cells was observed in all MDH laminae in KIG31-1–treated animals in comparison to those treated by Tat carrier. In the ipsilateral MDH, KIG31-1 significantly decreased the number of pERK1/2 cells in laminae I and II (IIi, IIo) only. Although KIG31-1 administration also decreased the number of pERK1/2-positive cells in the contralateral MDH, this increase was only significant in lamina II (IIi, IIo). *$P < .05$; **$P < .01$; ***$P < .001$.

preferentially low-threshold Aβ fibers, hence constituting a useful tool to investigate DMA.[39,40] Lamina III cells in the dorsal horn, which are known to receive Aβ primary afferent fibers,[41] may also become sensitized. In the present study, there was a significant increase in the staining and the number of positive PKCγ cells in lamina III of the MDH in CCI-IoN animals. MDH lamina III cells demonstrated a decrease in the expression of PKCγ to normal levels after intracisternal injection of vigabatrin, a drug that blocks the key enzyme for GABA degradation within the MDH.[15] Together, these observations suggest that the nociceptive behavior evoked in the present study by air-puff stimuli in CCI-IoN rats may have been due to the selective activation of Aβ fibers.

A Polysynaptic MDH Network Underlies Neuropathic Dynamic Mechanical Allodynia

The present study showed that ERK can be activated in MDH cells in response to innocuous stimuli (eg, air puffs) after trigeminal nerve injury. pERK1/2 expression may occur only in cells with neuronal features. The authors' previous study[7] and those of others[9,10] using double labeling with the neuronal marker NeuN have highlighted the neuronal subtype of pERK1/2-expressing cells. Remarkably, this ERK activation occurred in a manner tightly correlated with DMA severity. Indeed, nonstimulated neuropathic rats exhibited much less ERK1/2 activation, which could reflect the spontaneous pain-like behavior observed in CCI-IoN rats.[16] In line with this, the inhibition of DMA by the intracisternal administration of an ERK-signaling inhibitor has been reported in CCI-IoN rats.[13] ERK1/2 phosphorylation is known to promote central sensitization by regulating glutamate receptors and potassium channel activities.[12]

In the present study, the inhibition of PKCγ decreased the number of pERK1/2 cells within the MDH, and so possible projections between these two cells were investigated. PKCγ projections were observed in contact with pERK1/2 cells under light microscopy. The ultrastructural results confirmed the presence of PKCγ projections at the level of pERK1/2 cells and revealed synaptic contacts between the two cell subtypes. The PKCγ projections had the appearance of axonal processes, and most of them contacted pERK1/2-positive cells at the level of their cell bodies. Together, these data indicate that pERK1/2 cells may be activated directly through synaptic contacts from PKCγ cells which have been demonstrated to receive Aβ-fiber projections.[42] Therefore, the present findings suggest there is a preexisting linkage from the low-threshold Aβ mechanoreceptive pathway to the nociceptive pathway through PKCγ and pERK1/2 cell subtypes. This preexisting connection may be normally silent under physiologic conditions because it is under strong glycine or GABA inhibitory control. Once disinhibition occurs under pathologic conditions, the

circuitry composed of PKCγ and pERK1/2 may become active,[7,43,44] such that light mechanical stimulation activates lamina I cells through PKCγ–pERK1/2 cell connections.

Expression of PKCγ Is Enhanced in Neuropathic Rats

Consistent with previous studies,[4,6] CCI-IoN rats in the present study exhibited enhanced expression of PKCγ, especially in cells of laminae IIi and III. The PKCγ cells did not exhibit pERK1/2 expression after air-puff stimuli, as reported previously.[7] These observations underline the central role played by PKCγ cells in neuropathic DMA, relaying tactile information to nociceptive-specific pathways. This view is supported by the findings of the selective inhibition of segmental PKCγ with KIG31-1[40]: it reversed both the behavioral manifestations of DMA and the nociceptive neuronal activation induced by CCI-IoN. Indeed, in the present study, KIG31-1 considerably attenuated pERK1/2 expression not only in lamina I cells but also in lamina II cells, suggesting an action at the gate for tactile inputs. These results are in good agreement with studies where mice lacking PKCγ failed to develop tactile allodynia after sciatic nerve injury.[3]

A recent study has reported the inhibition of static mechanical allodynia in CCI-IoN rats after the administration of the nonselective PKC inhibitor chelerythrine.[6] However, the effects of chelerythrine seem to be related to multiple pharmacologic targets, including the inhibition of all PKC isoforms[40] and the glycine transporter 1 (GlyT1).[26] It is noteworthy that many isoforms of PKC have been implicated in neuropathic pain models[5,9] and that GlyT1 inhibition is known to reverse behavioral and cellular changes induced by nerve injury.[38] Thus, although in line with the present results, the effects of chelerythrine reported by Nakajima et al[6] cannot be ascribed to the specific inhibition of the PKCγ isoform.

Conclusions

This study has demonstrated a novel mechanism that could explain trigeminal DMA following CCI-IoN. It revealed a neuronal circuit activated during the DMA that is composed of at least two distinct cell subtypes: pERK1/2-positive cells and PKCγ cells. The latter are markedly recruited in DMA, as revealed by their upregulation of PKCγ molecules, which constitutes a key step in the sensitization of the MDH neuronal network composed of PKCγ and pERK1/2 cells. Inhibiting PKCγ in this circuit decreased the number of pERK1/2-positive cells and prevented DMA.

Acknowledgments

This work was funded by the Institut Nationale de la Santé et de la Recherche Médicale (INSERM) while the authors were members of INSERM U929. Wisam Dieb was supported by scholarships from the Institut Français pour la Recherche Odontologique (IFRO) and the Syrian Government. There are no conflicts of interest.

References

1. Zakrzewska JM, Lopez BC. Trigeminal neuralgia. Clin Evid 2006;15:1827–1835.
2. Polgár E, Fowler JH, McGill MM, Todd AJ. The types of neuron which contain protein kinase C gamma in rat spinal cord. Brain Res 1999;833:71–80.
3. Malmberg AB, Chen C, Tonegawa S, Basbaum AI. Preserved acute pain and reduced neuropathic pain in mice lacking PKC gamma. Science 1997;278:279–283.
4. Martin WJ, Liu H, Wang H, Malmberg AB, Basbaum AI. Inflammation-induced up-regulation of protein kinase C gamma immunoreactivity in rat spinal cord correlates with enhanced nociceptive processing. Neuroscience 1999;88:1267–1274.
5. Miletic V, Bowen KK, Miletic G. Loose ligation of the rat sciatic nerve is accompanied by changes in the subcellular content of protein kinase C beta II and gamma in the spinal dorsal horn. Neurosci Lett 2000;288:199–202.
6. Nakajima A, Tsuboi Y, Suzuki I, Honda K, Shinoda M, Kondo M, Matsuura S, Shibuta K, Yasuda M, Shimizu N, Iwata K. PKCgamma in Vc and C1/C2 is involved in trigeminal neuropathic pain. J Dent Res 2011;90:777–781.
7. Dieb W, Hafidi A. Mechanism of GABA-involvement in post-traumatic trigeminal neuropathic pain: Activation of neuronal circuitry composed of PKCγ interneurons and pERK1/2 expressing neurons. Eur J Pain 2014 May 28. doi: 10.1002/ejp.525 [Epub ahead of print].
8. Ji RR, Baba H, Brenner GJ, Woolf CJ. Nociceptive-specific activation of ERK in spinal neurons contributes to pain hypersensitivity. Nat Neurosci 1999;2:1114–1119.
9. Shimizu K, Asano M, Kitagawa J, Ogiso B, Ren K, Oki H, Matsumoto M, Iwata K. Phosphorylation of extracellular signal-regulated kinase in medullary and upper cervical cord neurons following noxious tooth pulp stimulation. Brain Res 2006;1072:99–109.
10. Hasegawa M, Kondo M, Suzuki I, Shimizu N, Sessle BJ, Iwata K. ERK is involved in tooth-pressure-induced Fos expression in Vc neurons. J Dent Res 2012;91:1141–1146.
11. Noma N, Tsuboi Y, Kondo M, et al. Organization of pERK-immunoreactive cells in trigeminal spinal nucleus caudalis and upper cervical cord following capsaicin injection into oral and craniofacial regions in rats. J Comp Neurol 2008;507:168–1440.
12. Ji RR, Gereau RW 4th, Malcangio M, Strichartz GR. MAP kinase and pain. Brain Res Rev 2009;60:135–148.
13. Lim EJ, Jeon HJ, Yang GY, et al. Intracisternal administration of mitogen-activated protein kinase inhibitors reduced mechanical allodynia following chronic constriction injury of infraorbital nerve in rats. Prog Neuropsychopharmacol Biol Psychiatry 2007;31:1322–1329.
14. Suzuki I, Tsuboi Y, Shinoda M, et al. Involvement of ERK phosphorylation of trigeminal spinal subnucleus caudalis neurons in thermal hypersensitivity in rats with infraorbital nerve injury. PLoS One 2013;8(2):e57278.

15. Dieb W, Hafidi, A. Astrocytes are involved in trigeminal dynamic mechanical allodynia: Potential role of D-serine. J Dental Res 2013;92:808–813.
16. Vos BP, Strassman AM, Maciewicz RJ. Behavioral evidence of trigeminal neuropathic pain following chronic constriction injury to the rat's infraorbital nerve. J Neurosci 1994;14:2708–2723.
17. Fischer L, Parada CA, Tambeli CH. A novel method for subarachnoid drug delivery in the medullary region of rats. J Neurosci Meth 2005;148:108–112.
18. Mao J, Price DD, Phillips LL, Lu J, Mayer DJ. Increases in protein kinase C gamma immunoreactivity in the spinal cord dorsal horn of rats with painful mononeuropathy. Neurosci Lett 1995;198:75–78.
19. Paxinos G, Watson C. The Rat Brain in Stereotaxic Coordinates. New York: Academic Press, 1997.
20. Decourt B, Hillman D, Bouleau Y, Dulon D, Hafidi A. Is otospiralin inner ear specific? Evidence for its expression in mouse brain. Int J Dev Neurosci 2009;27:87–96.
21. Martin YB, Malmierca E, Avendaño C, Nuñez A. Neuronal disinhibition in the trigeminal nucleus caudalis in a model of chronic neuropathic pain. Eur J Neurosci 2010;32:399–408.
22. Alvarez P, Dieb W, Hafidi A, Voisin DL, Dallel R. Insular cortex representation of dynamic mechanical allodynia in trigeminal neuropathic rats. Neurobiol Dis 2009;33:89–95.
23. Idänpään-Heikkilä JJ, Guilbaud G. Pharmacological studies on a rat model of trigeminal neuropathic pain: Baclofen, but not carbamazepine, morphine or tricyclic antidepressants, attenuates the allodynia-like behaviour. Pain 1999;79:281–290.
24. Shir Y, Seltzer Z. Effects of sympathectomy in a model of causalgiform pain produced by partial sciatic nerve injury in rats. Pain 1991;45:309–320.
25. Woda A, Pionchon P. A unified concept of idiopathic orofacial pain: Pathophysiologic features. J Orofac Pain 2000; 14:196–212.
26. Jursky F, Baliova M. Differential effect of the benzophenanthridine alkaloids sanguinarine and chelerythrine on glycine transporters. Neurochem Int 2011;58:641–647.
27. Koltzenburg M, Wall PD, McMahon SB. Does the right side know what the left is doing? Trends Neurosci 1999;22:122–127.
28. Ossipov MH, Lai J, Malan TP, Porreca F. Spinal and supraspinal mechanisms of neuropathic pain. Ann NY Acad Sci 2000;909:12–24.
29. Jacquin MF, Chiaia NL, Rhoades RW. Trigeminal projections to contralateral dorsal horn: Central extent, peripheral origins, and plasticity. Somatosens Mot Res 1990;7:153–183.
30. Panneton WM, Klein BG, Jacquin MF. Trigeminal projections to contralateral dorsal horn originate in midline hairy skin. Somatosens Mot Res 1991;8:165–173.
31. Colburn RW, Rickman AJ, DeLeo JA. The effect of site and type of nerve injury on spinal glial activation and neuropathic pain behavior. Exp Neurol 1999;157:289–304.
32. Winkelstein BA, Rutkowski MD, Sweitzer SM, Pahl JL, DeLeo JA. Nerve injury proximal or distal to the DRG induces similar spinal glial activation and selective cytokine expression but differential behavioral responses to pharmacologic treatment. J Comp Neurol 2001;439:127–139.
33. Sweitzer SM, Martin D, DeLeo JA. Intrathecal interleukin-1 receptor antagonist in combination with soluble tumor necrosis factor receptor exhibits an anti-allodynic action in a rat model of neuropathic pain. Neuroscience 2001;103:529–539.
34. Milligan ED, Twining C, Chacur M, et al. Spinal glia and proinflammatory cytokines mediate mirror-image neuropathic pain in rats. J Neurosci 2003;23:1026–1040.
35. Chiang CY, Dostrovsky JO, Iwata K, Sessle BJ. Role of glia in orofacial pain. Neuroscientist 2011;17:303–320.
36. Campbell JN, Raja SN, Meyer RA, Mackinnon SE. Myelinated afferents signal the hyperalgesia associated with nerve injury. Pain 1988;32:89–94.
37. Ochoa JL, Yarnitsky D. Mechanical hyperalgesias in neuropathic pain patients: Dynamic and static subtypes. Ann Neurol 1993;33:465–472.
38. Dohi T, Morita K, Kitayama T, Motoyama N, Morioka N. Glycine transporter inhibitors as a novel drug discovery strategy for neuropathic pain. Pharmacol Ther 2009;123:54–79.
39. Ahn DK, Jung CY, Lee HJ, Choi HS, Ju JS, Bae YC. Peripheral glutamate receptors participate in interleukin-1beta-induced mechanical allodynia in the orofacial area of rats. Neurosci Lett 2004;357:203–206.
40. Allen BJ, Li J, Menning PM, et al. Primary afferent fibers that contribute to increased substance P receptor internalization in the spinal cord after injury. J Neurophysiol 1999;81:1379–1390.
41. Brown AG, Rose PK, Snow PJ. Morphology of hair follicle afferent fibre collaterals in the cat spinal cord. J Physiol 1977; 272:770–797.
42. Basbaum AI, Bautista DM, Scherrer G, Julius D. Cellular and molecular mechanisms of pain. Cell 2009;139:267–284.
43. Torsney C, MacDermott AB. Disinhibition opens the gate to pathological pain signaling in superficial neurokinin 1 receptor-expressing neurons in rat spinal cord. J Neurosci 2006;26: 1833–1843.
44. Lu Y, Dong H, Gao Y, et al. A feed-forward spinal cord glycinergic neural circuit gates mechanical allodynia. J Clin Invest 2013; 123:4050–4062.